Since January 2020 Elsevier has created a COVID-19 resource centre with free information in English and Mandarin on the novel coronavirus COVID-19. The COVID-19 resource centre is hosted on Elsevier Connect, the company's public news and information website.

Antiviral Research 209 (2023) 105509

Contents lists available at ScienceDirect

Antiviral Research

journal homepage: www.elsevier.com/locate/antiviral

A new intracellular targeting motif in the cytoplasmic tail of the spike protein may act as a target to inhibit SARS-CoV-2 assembly

Longbo Hu [a,**,1], Yongjie Tang [a,1], Lingling Mei [a], Mengdi Liang [a], Jinxian Huang [a], Xufei Wang [a], Liping Wu [a], Jiajing Jiang [a], Leyi Li [a], Fei Long [a], Jing Xiao [a], Long Tan [a], Shaohua Lu [a], Tao Peng [a,b,c,*]

[a] State Key Laboratory of Respiratory Disease, Sino-French Hoffmann Institute, School of Basic Medical Science, Guangzhou Medical University, Guangzhou, 511436, China
[b] Guangdong South China Vaccine, Guangzhou, China
[c] Greater Bay Area Innovative Vaccine Technology Development Center, Guangzhou International Bio-island Laboratory, China

ARTICLE INFO

Keywords:
SARS-CoV-2
Spike protein
Cytoplasmic tail
Assembly
Intracellular targeting signal

ABSTRACT

Infection with severe acute respiratory syndrome coronavirus 2 (SARS-CoV-2) poses a threat to global public health, underscoring the urgent need for the development of preventive and therapeutic measures. The spike (S) protein of SARS-CoV-2, which mediates receptor binding and subsequent membrane fusion to promote viral entry, is a major target for current drug development and vaccine design. The S protein comprises a large N-terminal extracellular domain, a transmembrane domain, and a short cytoplasmic tail (CT) at the C-terminus. CT truncation of the S protein has been previously reported to promote the infectivity of SARS-CoV and SARS-CoV-2 pseudoviruses. However, the underlying molecular mechanism has not been precisely elucidated. In addition, the CT of various viral membrane glycoproteins play an essential role in the assembly of virions, yet the role of the S protein CT in SARS-CoV-2 infection remains unclear. In this study, through constructing a series of mutations of the CT of the S protein and analyzing their impact on the packaging of the SARS-CoV-2 pseudovirus and live SARS-CoV-2 virus, we identified $V_{1264}L_{1265}$ as a new intracellular targeting motif in the CT of the S protein, that regulates the transport and subcellular localization of the spike protein through the interactions with cytoskeleton and vesicular transport-related proteins, ARPC3, SCAMP3, and TUBB8, thereby modulating SARS-CoV-2 pseudovirus and live SARS-CoV-2 virion assembly. Either disrupting the $V_{1264}L_{1265}$ motif or reducing the expression of ARPC3, SCAMP3, and TUBB8 significantly repressed the assembly of the live SARS-CoV-2 virion, raising the possibility that the $V_{1264}L_{1265}$ motif and the host responsive pathways involved could be new drug targets for the treatment of SARS-CoV-2 infection. Our results extend the understanding of the role played by the S protein CT in the assembly of pseudoviruses and live SARS-CoV-2 virions, which will facilitate the application of pseudoviruses to the study of SARS-CoV-2 and provide potential strategies for the treatment of SARS-CoV-2 infection.

1. Introduction

The ongoing coronavirus disease 2019 (COVID-19) pandemic, caused by severe acute respiratory syndrome coronavirus 2 (SARS-CoV-2), has led to numerous cases of infection and death, and poses a great threat to human health (Sachs et al., 2022). SARS-CoV-2, as a member of the genus *Betacoronavirus* of the *Coronaviridae* family, is an enveloped, positive-sense RNA virus with a genome of approximately 29.8 kB, encoding sixteen nonstructural proteins (nsp1-nsp16), nine accessory proteins and four structural proteins: spike (S) protein, envelope (E) protein, matrix (M) protein, and nucleocapsid (N) protein (Bai et al., 2022). Among them, the S protein plays the essential role on the virus

* Corresponding author. State Key Laboratory of Respiratory Disease, Sino-French Hoffmann Institute, School of Basic Medical Science, Guangzhou Medical University, Guangzhou, 511436, China.
** Corresponding author.
E-mail addresses: longbo_hu@aliyun.com (L. Hu), peng_tao@gibh.ac.cn (T. Peng).
[1] Longbo Hu and Yongjie Tang contributed equally to this work.

https://doi.org/10.1016/j.antiviral.2022.105509
Received 31 October 2022; Received in revised form 19 December 2022; Accepted 21 December 2022
Available online 24 December 2022

entry, through mediating the binding of the virus to angiotensin-converting enzyme 2 (ACE2) on the host cell membrane and subsequent membrane fusion. Thus, the S protein is a significant target for current drug development and vaccine design against SARS-CoV-2. The S protein is a type I transmembrane protein. In structure, it comprises a large N-terminal extracellular domain, a transmembrane domain (TMD) and a short cytoplasmic tail (CT) at the C-terminus. The large N-terminal extracellular domain is composed of the S1 subunit responsible for receptor binding and the S2 subunit responsible for membrane fusion. However, the function of CT domain of S protein is poorly understood.

Previous studies have highlighted that the CT of viral membrane glycoproteins of other viruses facilitates the packaging of virus particles through assisting in maintaining proper subcellular trafficking and localization of glycoproteins. For instance, the CT of human immunodeficiency virus type 1 (HIV-1) envelope protein gp41 interacts with the Gag protein, which contribute to the enrichment of gp41 at the viral packaging site for subsequent efficient packaging into viral particles (Muranyi et al., 2013; Postler and Desrosiers, 2013; Roy et al., 2013; Tedbury and Freed, 2015). In addition, the interactions between the CT of the HA protein or NA protein of influenza A virus and the M1 protein facilitate the maintenance of the correct subcellular localization and packaging of viral particles (Barman et al., 2004; Jin et al., 1997; Kordyukova et al., 2021). Moreover, the CT of respiratory syncytial virus

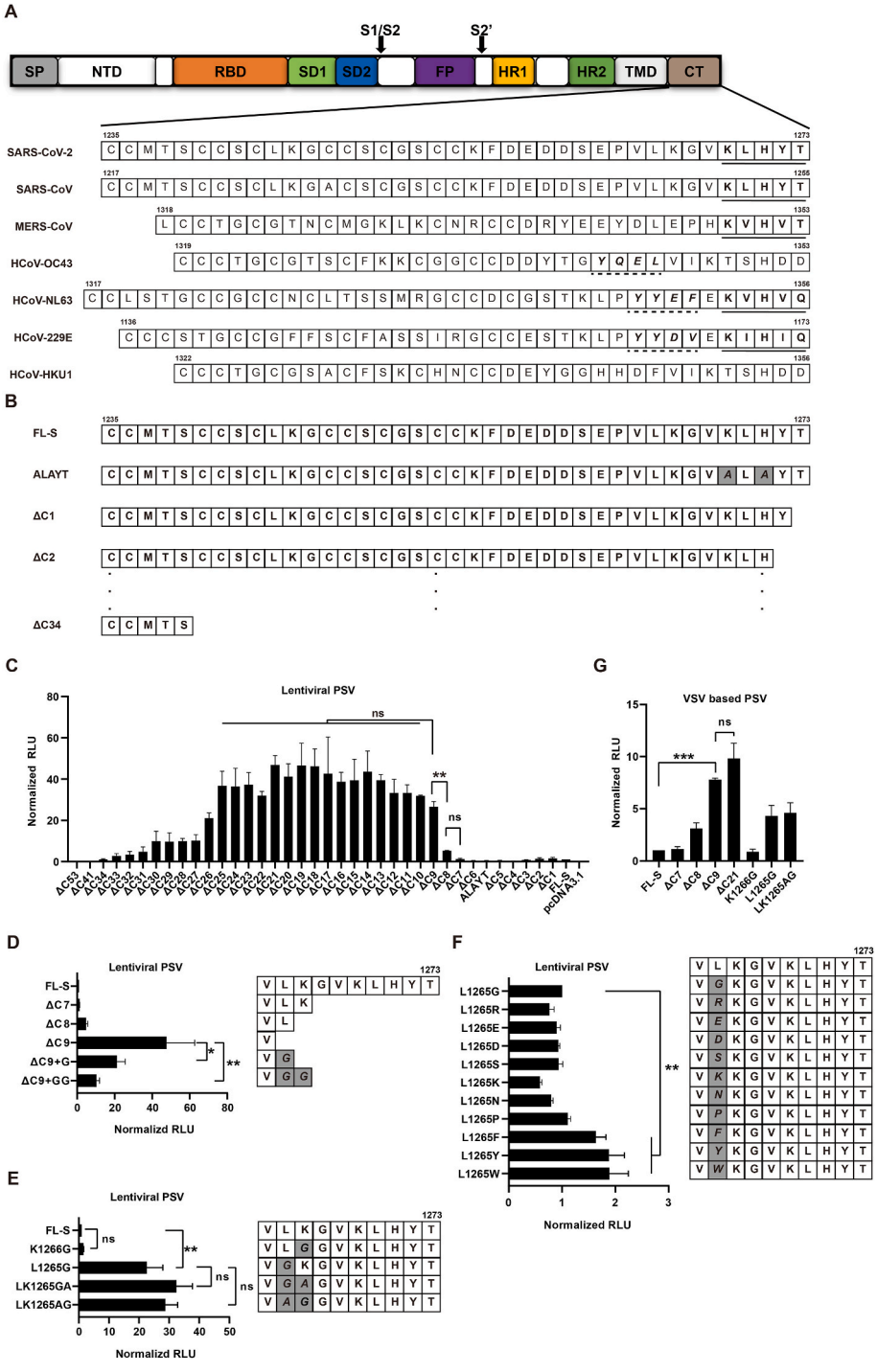

Fig. 1. L_{1265} in the cytoplasmic tail of the S protein is crucial for SARS-CoV-2 pseudovirus packaging. (A) Schematic diagram of the structure of the SARS-CoV-2 spike protein and the cytoplasmic tail sequences of human coronavirus (hCoV). The positions of the starting and ending amino acids of the cytoplasmic tail are annotated. Solid underlined bold and dashed underlined bold italics indicate the KxHxx motif and YxxΦ motif, respectively. SP, signal sequence; NTD, N-terminal domain; RBD, receptor-banding domain; SD1, subdomain 1; SD2, subdomain 2; S1/S2, protease cleavage site; S2′, protease cleavage site; FP, fusion peptide; HR1, heptad repeat 1; HR2, heptad repeat 2; TMD, transmembrane domain; CT, cytoplasmic tail. **(B)** A diagram showing the cytoplasmic tail sequence of the wild-type (FL-S), CT-truncated and ERRS-mutated (ALAYT) S protein. **(C)** 293T-ACE2 cells were infected with equal volumes of lentiviral pseudovirus carrying wild-type S (FL-S), CT-truncated or ERRS-mutated (ALAYT) S protein. To quantify the infection, luciferase activity was measured at 48 h post infection and normalized to that of the cells infected by the pseudovirus carrying FL-S. **(D–F)** The cytoplasmic tail of the S protein was truncated or mutated as indicated. 293T-ACE2 cells were infected with lentiviral SARS-CoV-2 pseudovirus bearing wild-type or mutated S proteins. Luciferase activity was measured at 48 h post infection and normalized to that of the cells infected with the pseudovirus bearing FL-S (**D** and **E**) or the L1265G mutant (**F**). **(G)** Vesicular stomatitis virus (VSV)-based SARS-CoV-2 pseudovirus carrying the indicated wild-type or mutant S protein was prepared by transient transfection of HEK293T cells with an S protein-expressing plasmid followed by infection with G*ΔG-VSV. 293T-ACE2 cells were infected with VSV-based SARS-CoV-2 pseudovirus. The infection was then measured by firefly luciferase activity at 48 h post-infection and normalized to that of the cells infected by pseudovirus bearing wild type S. Data are shown as the mean ± SEM (standard error of the mean) of at least three independent experiments. PSV, pseudovirus; ns, no significance; *, $p < 0.05$; **, $p < 0.01$; ***, $p < 0.001$.

fusion protein mediates virion assembly through incorporation of internal virion proteins into virus filaments at the cell surface (Baviskar et al., 2013; Shaikh et al., 2012). For most coronaviruses, the S protein has a cytoplasmic tail of approximately 40 amino acids, that modulates the intracellular transport and subcellular localization of the S protein through one or two classic intracellular targeting motifs: a tyrosine-based sorting motif, YxxΦ (x is any residue and Φ is a bulky hydrophobic residue), and/or an ER retrieval signal (ERRS), KxHxx/KKxx motif (Fig. 1A) (Hou et al., 2019). However, there is no YxxΦ motif in the CT of SARS-CoV and SARS-CoV-2 S proteins. Furthermore, the KxHxx motif (KLHYT) in SARS-CoV and SARS-CoV-2 S protein has been identified as a weak and suboptimal ER retrieval motif that cannot efficiently mediated S protein retention in the ER (Jennings et al., 2021; Lontok et al., 2004; McBride et al., 2007; Ujike et al., 2016). Therefore, it is speculated that there may be other intracellular localization signals in the CT of the SARS-CoV and SARS-CoV-2 S proteins.

Since live SARS-CoV-2 research is restricted to biosafety level 3 (BSL-3) laboratories, the research and development of SARS-CoV-2 vaccines and antiviral drugs has been severely impeded. Thus, the pseudoviruses (PSVs) based on vesicular stomatitis virus (VSV) or HIV-1 virions pseudotyped with the SARS-CoV-2 S protein are useful alternative approaches that can mimic the entry process of SARS-CoV-2 and be utilized to screen and evaluate antivirals and vaccine candidates safely and effectively at BSL-2 laboratory (Chen and Zhang, 2021; Salazar-Garcia et al., 2021; Xiang et al., 2022a). Previous studies have shown that CT truncation of the S protein can enhance the infectivity of SARS-CoV and SARS-CoV-2 pseudovirus (PSV), which is speculated due to the deletion of ERRS (Chen et al., 2021; Giroglou et al., 2004; Johnson et al., 2020; Moore et al., 2004; Yu et al., 2021). However, the number of amino acids truncated in the CT varies from study to study, and the underlying molecular mechanism has not been precisely elucidated. In-depth insight into the role of the CT in the packaging of SARS-CoV-2 PSV will considerably facilitate the application of pseudoviruses in the research and development on therapeutic agents and vaccines for SARS-CoV-2 and related human coronaviruses. In addition, the precise role of the CT of the S protein in SARS-CoV-2 infection remains unclear, and its elucidation will also enhance the understanding of the viral infection process and shed new light on the design of improved diagnosis and treatment programs.

In this study, we identified a novel intracellular targeting motif in the CT of the SARS-CoV and SARS-CoV-2 S protein, $V_{1264}L_{1265}$, which interacted with the cytoskeleton and vesicle transport-related proteins to regulate the intracellular transport of S protein, and thereby modulated incorporation of S protein into pseudovirus particles and live SARS-CoV-2 virions. Notably, knocking down CT-interacting proteins significantly blunted the assembly of SARS-CoV-2 virion, suggesting its potential as a new drug target. Our findings shed light on the crucial role of the CT of the S protein in SARS-CoV-2 infection and provide insights into potential drug targets against SARS-CoV-2 infection.

2. Material and methods

2.1. Cells and reagents

HeLa and HEK293T cells were cultured in DMEM supplemented with 10% FBS, 100 unit/mL penicillin and 100 μg/mL streptomycin at 37 °C and 5% CO_2 incubator. All cell lines were negative for contamination with mycoplasma. The 293T-hACE2 cell line stably expressing human angiotensin-converting enzyme 2 (ACE2) was generated by lentiviral transduction of human ACE2 into HEK293T cells, followed by stable cell selection using 2 μg/mL puromycin. The antibody against VSV M (P04876) was purchased from CUSABIO (China), the antibodies against Gag protein(ab9071) and HA tag (ab9110) were purchased from Abcam (USA), the antibody against GAPDH (KC-5G5) was purchased from KANGCHEN (China), and the anti-FLAG antibody (F1804) was purchased from Sigma (USA).

2.2. Plasmid construction

The full-length of spike gene of SARS-CoV-2 Wuhan-Hu-1 strain (GenBank: MN908947) was codon-optimized, synthesized and cloned into pcDNA3.1(+) vector between BamH I and EcoR I sites of the to generate pcDNA3.1(+)-FL-S (FL-S). Cytoplasmic tail truncation- and sequence-related mutations were constructed by PCR or site-directed mutagenesis according to the manufacturer's instructions. All constructed plasmids were verified by sequencing.

2.3. Preparation of pseudotyped viruses

Lentivirus based SARS-CoV-2 pseudoviruses were prepared using the methods described in our previous study (Hu et al., 2022). In brief, HEK293T cells were co-transfected with a construct expressing viral envelope protein, a lentiviral vector (pWPXL) expressing firefly luciferase reporter protein and a lentiviral packaging plasmid (psPAX2) using Lipofectamine 3000 transfection reagent (Invitrogen). The supernatants were refreshed by prewarmed DMEM at 6–8 h post-transfection and harvested at 48 h post-transfection, followed by passage through a 0.45 μm low protein binding filter, and then kept at −80 °C. Vesicular stomatitis virus (VSV) based SARS-CoV-2 pseudoviruses were produced as previously described (Nie et al., 2020). Briefly, HEK293T cells were transfected with plasmids encoding wild-type or mutant S proteins. The transfected cells were infected with G*ΔG-VSV (VSV G pseudotyped virus) at 24 h post-transfection at an MOI of 0.05. Supernatants were refreshed at 2 h post infection and harvested at 24 h post infection, filtered through a 0.45 μm low protein binding filter, and then stored at −80 °C. To further purify and concentrate SARS-CoV-2 pseudovirus, the virus-containing supernatants were subjected to centrifugation at 10,000 rpm for 30 min to remove cell debris, followed by ultracentrifugation at 100,000×*g* for 3 h using an SW-32 rotor. The supernatant was removed, and the virus pellet was resuspended in PBS, aliquoted and stored at −80 °C.

2.4. SARS-CoV-2 spike-based cell fusion assay

The SARS-CoV-2 spike-based cell fusion assay was performed as previously described with slight modification (Peng, 2010). HEK293T cells co-transfected with plasmids encoding hACE2 and T7 RNA polymerase (pRNP; kindly provided by Dr Richard Longnecker of Northwestern University) were used as target cells. HEK293T cells co-transfected with plasmids encoding SARS-CoV-2 S protein and the firefly luciferase gene driven by a T7 promoter (pT7Luc; kindly provided by Dr Richard Longnecker of Northwestern University) were used as effector cells. The effector and target cells were dissociated by trypsin (Invitrogen, USA) and mixed in equal proportions for co-culture at 72 h post transfection. The luciferase activity was assessed after 24 h of incubation.

2.5. Real-time quantitative PCR (RT-qPCR)

Quantification of viral RNA levels in cells and culture supernatants was performed by RT-qPCR. To measure the viral RNA level in cell culture supernatants, viral RNA was extracted from virus-containing supernatant using a QIAamp Viral RNA Mini Kit (Qiagen), as described in the manufacturer's protocol. To detect the viral RNA level in cells, total cellular RNA was extracted using a UNlQ-10 total RNA isolation Kit (B511361, Sangon Biotech, Shanghai, China). cDNA was synthesized using a cDNA reverse transcription kit (EP0451, Thermo Scientific) according to the manufacturer's instructions and subjected to qPCR analysis using a fluorescence quantitative PCR instrument (CFX96, Bio-Rad, San Diego, CA, USA). Primers against SARS-CoV-2 subgenomic RNA (5′-CCTTCCCAGGTAACAAACCAACC-3′/5′-CAGTATTATTGGGTAAACCTTGGGGC-3′) (Jin et al., 2021) were used to quantify the intracellular SARS-CoV-2 RNA level; primers against gag gene

(5′-TTCGGTTAAGGCCAGGGG-3′/5′-CTTCTGATCCTGTCTGAAGGG-3′) were used to quantify the supernatant lentiviral RNA expression level; primers against the L gene (5′-AATGACGATGAGACYATGCAATC-3′/5′-CAAGTCACYCGTGACCATCT-3′) were used to quantify the supernatant VSV RNA expression level. For absolute quantification of supernatant lentiviral and VSV RNA expression levels, serial dilutions of plasmids encoding gag and L proteins were used as standards in qPCR, respectively.

2.6. Co-immunoprecipitation/mass spectrometry (Co-IP/MS)

The intracellular proteins interacting with the CT of the S protein in lentiviral and VSV-based pseudovirus packaging cells were identified using immunoprecipitation and mass spectrometry. For lentiviral PSV packaging system, HEK293T cells were co-transfected with pWPXL, psPAX2 and plasmids expressing GFP, GFP-CT or GFP-CT-ΔC9, respectively. At 48 h post transfection, cells were harvested and processed for sequential anti-FLAG immunoprecipitation. For VSV-basde PSV packaging system, HEK239T cells were transfected with plasmids expressing GFP, GFP-CT or GFP-CT-ΔC9, respectively, and infected with G*ΔG-VSV (VSV G pseudotyped virus) at 24 h post transfection at an MOI of 0.05. At 24 h post infection, cells were harvested and processed for sequential anti-FLAG immunoprecipitation. The immunoprecipitation and the subsequent mass spectrometry (MS) analysis were performed using a Pierce MS-Compatible Magnetic IP Kit (Thermo Scientific) following the manufacturer's instructions. In brief, cells were lysed in IP-MS Cell Lysis Buffer on ice for 10 min and centrifuged at ~13,000×*g* for 10 min. The supernatant was collected and mixed with 5 μg of anti-FLAG antibody (M2, Sigma). After the overnight incubation at 4 °C, protein A/G magnetic beads were added to the lysate/antibody mixture and incubated for 1 h at room temperature, followed by rinse with IP-MS wash buffer and sequential elution with IP-MS elution buffer. The elution was dried and resuspended in 6 M urea/50 mM triethylammonium bicarbonate (TEAB), and incubated with Tris (2-carboxyethyl) phosphine (TCEP) at 37 °C for 30 min. Iodoacetamide (IAA) was then added to the sample and incubated at room temperature for 30 min, followed by the digestion with trypsin overnight at 37 °C. The sample was then mixed with 10% trifluoroacetic acid (TFA) and centrifuged at 15,000×*g* for 2 min. The supernatant was cleaned up with a C18 trap column and processed for MS analysis using Q Exactive Orbitrap Mass Spectrometers (Thermo Scientific). The raw data were acquired and processed with MaxQuant software with default settings referencing the Uniprot database. The Co-IP/MS experiments were repeated twice, and only proteins identified in both independent replicates were included in subsequent analyses (Table S1).

2.7. Immunofluorescence analysis (IFA)

HeLa cells that transfected with plasmid DNA encoding different spike mutants using Lipofectamine 3000 were seeded on glass coverslips 48 h after transfection in a humidified incubator at 37 °C with 5% CO2. Twenty-four hours after seeding, the cells were washed with PBS, fixed in 4% paraformaldehyde for 20 min at room temperature and then incubated in QuickBlock buffer (Beyotime) for 10 min. The cells were washed and incubated with a rabbit polyclonal antibody against spike protein (1:400) for 1 h, followed by staining with AF555-conjugated goat anti-rabbit IgG (1:500) to detect the cell-surface spike protein. Cells were subsequently washed five times in PBS and permeabilized with Triton, followed by incubation in QuickBlock buffer (Beyotime) for 10 min. Then, the cells were washed and incubated with a rabbit polyclonal antibody against spike protein (1:400) for 1 h, followed by staining with AF488-conjugated goat anti-rabbit IgG (1:500) to label the intracellular spike protein (as well as available cell-surface S protein). After counterstaining the nuclei with DAPI, the cells were mounted in Dako Fluorescent Mounting Medium (S3023) and imaged using a Leica TCS SP8 confocal microscope equipped with Leica Application Suite X software.

2.8. Generation of single-round infectious SARS-CoV-2

The single-round infectious SARS-CoV-2 virion was generated by the SARS-CoV-2 replicon with the deletion of the spike gene (Jin et al., 2021) (kindly provided by Professor Ji-An Pan from Sun Yat-sen University) trans-complemented with ectopically expressing the spike protein according to the protocols described in a previous study (Ricardo-Lax et al., 2021) with slight modifications. Briefly, HEK293T cells (1.5×10^6) were plated into 6-cm dishes 24 h before transfection, and then co-transfected with 3 μg plasmid encoding spike protein and 3 μg SARS-CoV-2 replicon RNA. The medium was refreshed 6–8 h after transfection and virus-containing supernatants were collected 48 h after transfection, centrifuged to remove debris, and used to infect 293T-ACE2 cells.

2.9. Flow cytometry

HEK293T cells were transfected with plasmids expressing spike proteins using Lipofectamine 3000. Cells were harvested and rinsed twice with wash buffer (1% FBS in PBS), and then fixed for 15 min with 4% paraformaldehyde. To detect spike protein on the cell surface, cells were incubated with rabbit polyclonal antibody against spike protein (1:400) for 30 min at room temperature, followed by staining with AF488-conjugated goat anti-rabbit IgG (1:500) (Invitrogen A11008) for 30 min, and then analyzed by flow cytometry using an Accuri C6 instrument (BD Biosciences). For the detection of the intracellular and cell-surface spike protein, cells were permeabilized with 0.1% Triton prior to primary antibody incubation.

2.10. Sequence data

Mutations occurrence data were downloaded from the GISAID database (https://gisaid.org/hcov19-mutation-dashboard/) in August 2022 (Elbe and Buckland-Merrett, 2017). The amino acid sequence of isolate Wuhan-Hu-1 was used as the reference proteome (GenBank accession no. MN908947).

2.11. Statistical analysis

All experiments were performed at least three times. The data were presented as mean ± SD(SEM). Statistical significance was analyzed by Student's *t*-test or one-way ANOVA statistical tests where appropriate using GraphPad Prism 8. $p < 0.05$ was considered statistically significant. ($^{*}p < 0.05$, $^{**}p < 0.01$, $^{***}p < 0.001$, $^{****}p < 0.0001$).

3. Results

3.1. L_{1265} in the cytoplasmic tail of the SARS-CoV-2 spike protein is crucial for the enhanced infectivity of SARS-CoV-2 pseudovirus

To determine the effect of CT deletion on SARS-CoV-2 pseudovirus packaging, we constructed a series of CT truncation mutants by deleting the amino acids of CT one by one (ΔC1 to ΔC34 in Fig. 1B) from full-length wild-type spike protein (FL-S) and compared the infectivity of pseudoviruses (PSVs) packaged by these mutants using a lentiviral packaging system. Previous studies have attributed the promotion of SARS-CoV pseudovirus infectivity by CT deletion to the deletion of putative ER retrieval signal (ERRS) located in the last 5 amino acids (KLHYT) of the CT, but our results indicated that neither deletion of ERRS (ΔC5) nor mutation of ERRS (ALAYT) significantly enhanced the infectivity of SARS-CoV-2 pseudovirus (Fig. 1C). The infectivity of SARS-CoV-2 pseudovirus was significantly increased when the last 9 amino acids in the CT of the S protein were removed (ΔC9) (Fig. 1C). Compared with ΔC9, further deletions of amino acids (ΔC10 to ΔC26) did not

significantly improve the infectivity of SARS-CoV-2 pseudoviruses, indicating that the last 9 amino acids of the spike protein were the determining factor for SARS-CoV-2 pseudovirus packaging (Fig. 1C). Moreover, the length of the CT seemed critical to the package of SARS-CoV-2 pseudovirus, since the infectivity of SARS-CoV-2 PSVs was markedly reduced when one or two glycine residues were added at the COOH-terminus of ΔC9 (Fig. 1D). In order to figure out which amino acids in CT determine SARS-CoV-2 pseudovirus packaging efficiency, we substituted the L1265 and K1266 individually or simultaneously with glycine or alanine in FL-S and detected the infectivity of SARS-CoV-2 PSV. As shown in Fig. 1E, the infectivity of SARS-CoV-2 PSV was significantly increased when L1265 was substituted with glycine, but the substitution of K1266 with glycine had no effect on the infectivity of SARS-CoV-2 PSV. These results suggested the critical role of L1265 on the efficient SARS-CoV-2 PSV packaging. Then, we wondered whether the chemical properties of the amino acid at position 1265 had any influence on SARS-CoV-2 PSV packaging. Therefore, we substituted L1265 with amino acids with different chemical properties, including positively charged (Lys or Arg), negatively charged (Asp or Glu), aromatic (Phe, Tyr or Trp) and polar uncharged (Ser or Asn), and tested the infectivity of packaged SARS-CoV-2 PSV. As shown in Fig. 1F, the packaged SARS-CoV-2 PSV displayed highest infectivity only when the L1265 was replaced by the aromatic amino acids. Consistent results were obtained in the vesicular stomatitis virus (VSV)-based PSV packaging system, indicating that the enhancement of SARS-CoV-2 PSV infectivity through the truncation of the last 9 amino acids or the substitution of L1265 in the spike protein on was independent of the packaging system (Fig. 1G).

3.2. CT truncation of the spike protein enhances its incorporation in the SARS-CoV and SARS-CoV-2 pseudovirus by increasing its cellular surface localization

Our results suggested that the truncation of the last 9 amino acids of the spike protein significantly promoted the SARS-CoV-2 PSV packaging. Next, we sought to elucidate the underlying mechanism of this promotion. Since the S protein mediates the receptor-binding and membrane fusion steps of viral entry, we first assessed the effect of CT truncation on the ability of the S protein to bind to the ACE2 receptor and mediate membrane fusion by a cell fusion assay. The transmembrane domain of S protein plays important role during entry (Broer et al., 2006; Corver et al., 2009). The mutants missing most or all transmembrane domains (ΔC41 or ΔC53) partially or completely lost its membrane localization, rendering it incapable of mediating membrane fusion as the expectation, indicating the reliability of this assay to study the membrane fusion (Fig. 2A). Compared with FL-S protein, CT truncations did not display enhanced fusion activity (Fig. 2A). Then, we detected the expression levels of spike proteins in SARS-CoV-2 pseudovirus particles. The mutants with the last 9 or 21 amino acids truncations, as well as the mutants with L1265 substitutions exhibited much

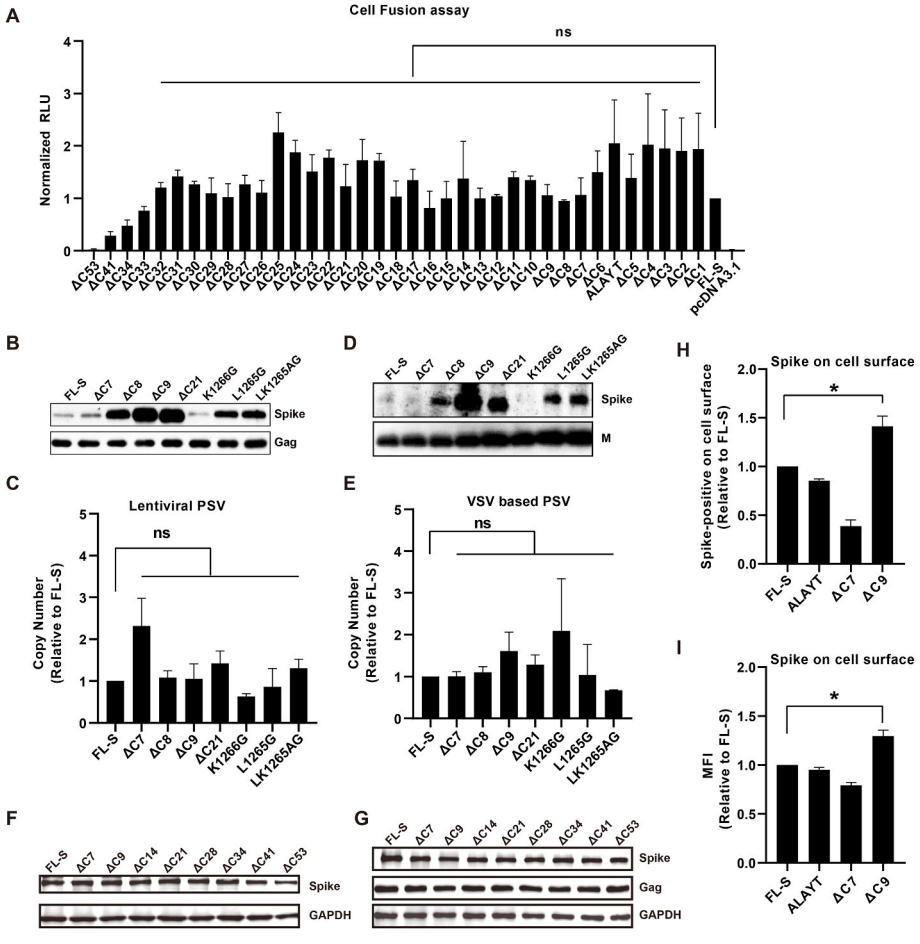

Fig. 2. CT truncation promoted incorporation of SARS-CoV-2 S protein into pseudovirus particles by increasing their expression on the cell surface. (A) A cell fusion assay was performed to assess the ability of wild-type and CT-truncated S proteins to mediate receptor binding and subsequent membrane fusion. HEK293T cells co-transfected with pT7Luc and plasmids encoding S protein were mixed at a 1:1 ratio with those cells co-transfected with pRNP and plasmid expressing hACE2 at 72 h after transfection. The luciferase activity in the cell lysates was determined and normalized to hACE2 mixed with wild-type S protein. **(B–E)** Lentiviral PSVs and VSV-based PSVs bearing wild-type or mutant SARS-CoV-2 S protein were concentrated by ultracentrifugation. The S protein expression level in lentiviral PSV **(B)** or VSV-based PSV **(D)** were detected by Western blot, and the viral structure protein Gag or M was used as an internal control. The viral genomic copy numbers of concentrated lentiviral PSV **(C)** and VSV-based PSV **(E)** were quantified by RT-qPCR and normalized to FL-S. Serial dilutions of plasmids encoding the HIV-1 gag gene or VSV L gene were used as standards, respectively. **(F–G)** HEK293T cells were transfected with plasmids encoding the wild-type or CT truncated S protein **(F)** or co-transfected with lentiviral packaging plasmids (pWPXL and pSPAX2) and plasmids encoding the wild-type or CT truncated S protein **(G)**. The S protein expression levels were measured by Western blot at 48 h after transfection. GAPDH and Gag protein expression were used as internal controls for loading and transfection efficiency. **(H–I)** HEK293T cells were co-transfected with lentiviral packaging plasmids and plasmids encoding wild-type or mutant SARS-CoV-2 S protein. The expression level of S protein on the cell surface was detected by flow cytometry using an anti-spike antibody at 48 h post transfection. The percentage of spike-positive cells **(H)** and mean fluorescence intensity (MFI) **(I)** are represented and normalized to FL-S. Data are shown as the mean ± SEM (standard error of the mean) of at least three independent experiments. PSV, pseudovirus; ns, no significance; *, $p < 0.05$; ***, $p < 0.001$.

higher expression levels than the full-length S protein in SARS-CoV-2 PSV particles (Fig. 2B).

But no significant difference was detected in the lentiviral structure protein (Gag) as well as genomic RNA levels among CT truncated mutants and FL-S packaged lentiviral pseudovirions (Fig. 2B and C). Similar results were observed in the VSV-based PSV packaging system (Fig. 2D and E). These results suggested that the last 9 amino acid truncation or the L1265 substitution did not affect the number of lentiviral pseudovirus particles but promoted the incorporation of spike protein into lentiviral pseudovirions.

Furthermore, the expression levels of S protein in the transfected cells or the PSV packaging was similar among the FL-S and CT truncated S protein (Fig. 2F and G), suggesting that CT truncations did not increase the S protein in SARS-CoV-2 PSV through directly increasing the expression level of S protein. Since lentiviruse and VSV virions acquire their envelope glycoproteins and bud at the plasma membrane (Freed, 2015; Lyles, 2013), we speculated that the CT truncation facilitates the incorporation of the S protein into PSV by increasing its localization on the plasma membrane. Flow cytometric results indicated that the truncation of the last 9 amino acids of the spike protein significantly increased its localization on the plasma membrane (Fig. 2H and I). However, mutation or deletion of ERRS (ALAYT and ΔC7) did not affect the cell surface localization of the spike protein (Fig. 2H and I), further illustrating that ERRS is not a decisive factor in aiding SARS-CoV-2 pseudovirus packaging. Considering that the CT of the SARS-CoV and SARS-CoV-2 S protein is highly conserved (Fig. 1A), we speculated that the truncation of the last 9 amino acids of the SARS-CoV spike protein would promote the infectivity of SARS-CoV pseudoviruses such as SARS-CoV-2. As expected, the infectivity of the SARS-CoV PSV was significantly increased after truncation of the last 9 amino acids of the spike protein, while the deletion of additional amino acids failed to further enhance the infectivity (Fig. 3A). Consistently, the packaging efficiency of SARS-CoV S protein was also increased when the last 9 amino acids of the SARS-CoV spike protein was deleted, regardless of the packaging systems (Fig. 3B–E). Overall, these results suggested that deletion of the last 9 amino acids of the SARS-CoV-2 or SARS-CoV spike protein enhanced its incorporation into pseudovirus particles by increasing the plasma membrane localization of the spike protein.

3.3. ARPC3, SCAMP3 and TUBB8 participate in SARS-CoV-2 pseudovirus packaging through interactions with the CT of the spike protein

To further elucidate the key regions in the spike protein responsible for the efficient packaging of SARS-CoV-2 pseudovirus, we used FLAG-tagged GFP to replace the extracellular domain of S protein, and constructed FLAG-tagged GFP fused with the TMD and full-length CT of the S protein (GFP-CT) or with the TMD and the last 9 amino acids-truncated CT of the S protein (GFP-CT-ΔC9) (Fig. 4A). Then we packaged the pseudoviruses with these fusion proteins and detected the levels of GFP expression both in pseudovirus packaging cells and pseudovirus particles. Similar to that of the FL-S and ΔC9, no evident difference in the expression levels of the three fusion proteins was observed in pseudovirus packaging cells, but the expression level of GFP-CT-ΔC9 in pseudovirus particles was significantly higher than that of GFP-CT and GFP as a control. These results suggested that the truncation of the last 9 amino acids of CT could not only promote the incorporation of spike protein into pseudovirus particles but also facilitate the incorporation of GFP into pseudovirus particles, further confirming the key role of the last 9 amino acids in the SARS-CoV-2 PSV packaging (Fig. 4B and C). Next, in order to investigate the host proteins involved in the SARS-CoV2 PSV packaging, we performed immunoprecipitation coupled with mass spectrometry (IP-MS) and identified 280 GFP-CT interacting proteins, 141 GFP interacting proteins and 447 GFP-CT-ΔC9 interacting proteins in both lentiviral and VSV-based pseudovirus packaging cells (Table S1). Among them, there were 35 proteins specifically interacting with GFP-CT, 225 proteins specifically interacting with GFP-CT-ΔC9 and 8 proteins specifically interacting with GFP proteins, respectively (Fig. 4D). Since the deletion of the last 9 amino acids increased the incorporation efficiency of protein in pseudovirus particles (GFP-CT vs. GFP-CT-ΔC9 in Fig. 4C), we speculated that some protein interacting with GFP-CT and inhibited its packaging into pseudovirus particles, and as a result, initially focused on 35 proteins that specifically interact with GFP-CT. Protein–protein interaction (PPI) network and gene ontology (GO) analyses of the 35 GFP-CT-specific interacting proteins revealed enriched genes involved in cytoskeleton assembly (such as ARPC3 and TUBB8) and vesicular transport (such as SCAMP3) and functioning in actin/cytoskeleton protein binding and intracellular protein transport (Fig. 4E and F). Then, we knocked down these GFP-CT-specific interacting proteins in pseudovirus packaging cells to detect the impact of these proteins on the infectivity of FL-S- or ΔC9- packaged SARS-CoV-2 PSV (Fig. S1). Among these tested proteins, knocking down ARPC3, SCAMP3 and TUBB8 significantly enhanced the infectivity of FL-S-packaged pseudovirus but had no significant effect on the infectivity of the ΔC9-packaged pseudovirus (Fig. 4G). Then we performed a reciprocal co-IP assay to confirm that ARPC3, SCAMP3 and TUBB8 specifically interacted with GFP-CT, but not GFP and GFP-CT-ΔC9 (Fig. 4H). In addition, knockdown of ARPC3, SCAMP3 and TUBB8 expression significantly increased the localization of the full-length spike protein on the cell surface and increased the packaging efficiency of the full-length spike protein into SARS-CoV-2 PSV particles (Fig. 4I and J). Taken together, these results suggest that ARPC3, SCAMP3 and TUBB8 interact with the full-length CT of the spike protein and block its packaging into pseudovirus particles through suppressing its localization on the cell surface.

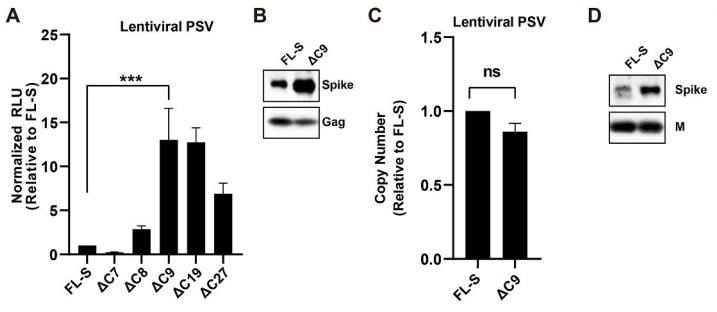

Fig. 3. CT truncation promoted incorporation of SARS-CoV S protein into pseudovirus particles. (A) The luciferase activity in 293T-ACE2 cells infected by lentiviral SARS-CoV pseudovirus carrying wild type or CT truncated S protein was measured at 48 h post infection and normalized to FL-S. The S protein expression level in lentiviral SARS-CoV pseudovirus **(B)** or VSV-based SARS-CoV pseudovirus **(D)** bearing wild type or the last nine amino acid deleted S protein (ΔC9) was detected by Western blot, and the viral structure protein gag or M was used as an internal control. The viral genomic copy numbers of concentrated lentiviral SARS-CoV PSV **(C)** and VSV-based SARS-CoV PSV **(E)** were quantified by RT-qPCR and normalized to FL-S. Serial dilutions of plasmids encoding the HIV-1 gag gene or VSV L gene were used as standards, respectively. Data are shown as the mean ± SEM (standard error of the mean) of at least three independent experiments. PSV, pseudovirus; ns, no significance. ***, $p < 0.001$.

3.4. $V_{1264}L_{1265}$ in the CT of the spike protein is essential for the assembly of SARS-CoV-2 virions

Unlike VSV and lentivirus virions whose assembly and release take place on the plasma membrane, the assembly of mature SARS-CoV-2 virions occurs within the ER-to-Golgi intermediate compartment (ERGIC) (Lebeau et al., 2020). Thus, we investigated the effect of CT truncation of the spike protein on the assembly of live SARS-CoV-2 virions utilizing single-round infectious SARS-CoV-2 virions produced by a trans-complementation system to mimic the assembly process of live SARS-CoV-2 virions.

The trans-complementation system consists of a SARS-CoV-2 replicon RNA containing spike gene deletion and a spike-encoding plasmid ectopically expressing the spike protein (Jin et al., 2021; Ricardo-Lax et al., 2021). There was no significant difference in the viral RNA expression levels in single-round infectious SARS-CoV-2 packaging cells, suggesting that the deletion of the last 9 amino acids of the spike protein did not affect the replication of the SARS-CoV-2 genome (Fig. 5A). However, the expression level of SARS-CoV-2 RNA in cells infected by ΔC9 packaged single-round infectious SARS-CoV-2 was significantly

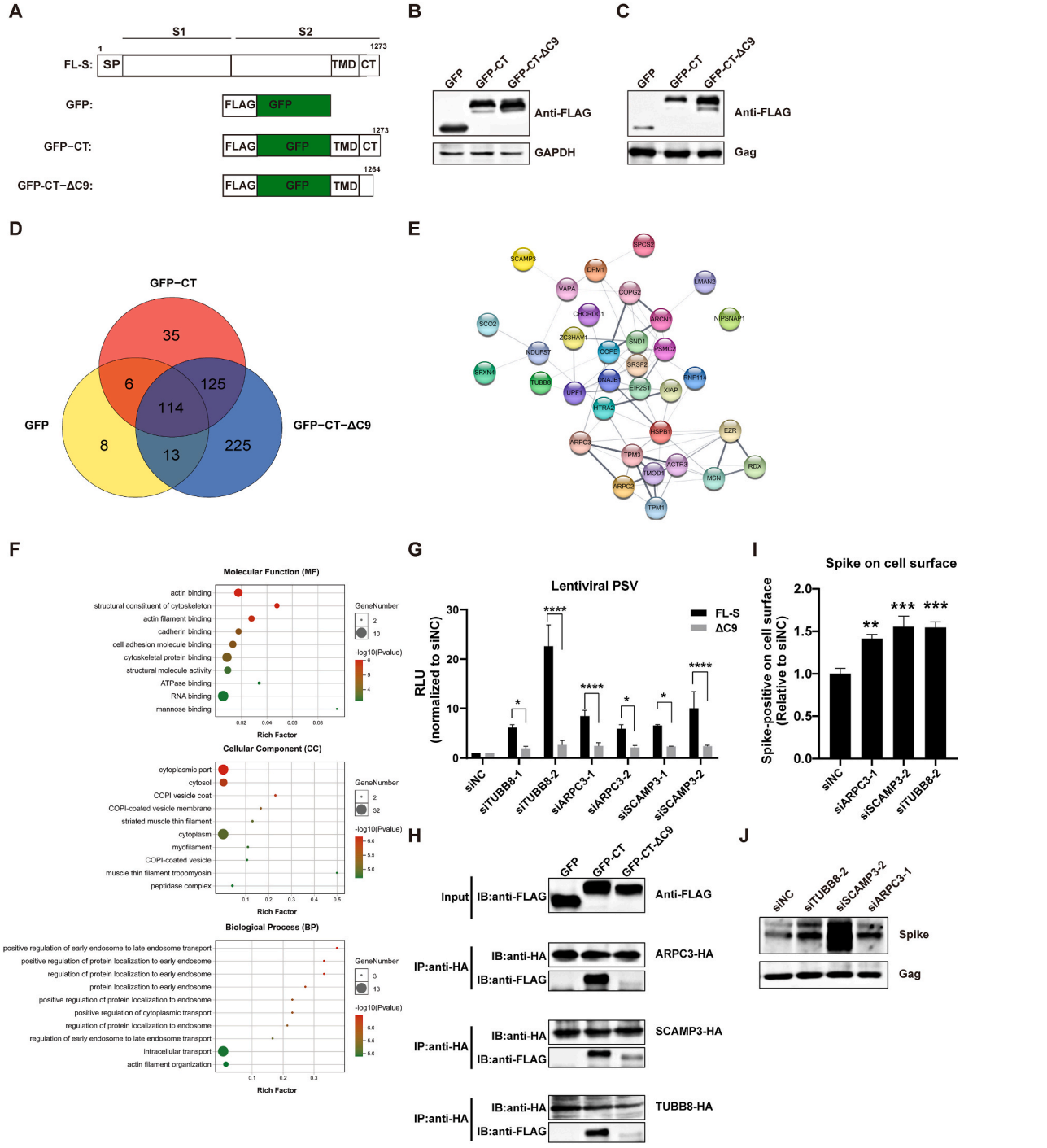

(caption on next page)

Fig. 4. Identification of CT-interacting proteins modulating intracellular transport of S protein and infectivity of SARS-CoV-2 pseudovirus. (A) Schematic diagram showing the protein structure of GFP fusion proteins: GFP, which comprises an N-terminal FLAG tag and GFP; GFP-CT, which comprises an N-terminal FLAG tag, followed by GFP, and the TMD as well as full-length CT of S; and GFP-CT-Δ9, which comprises an N-terminal FLAG tag, followed by GFP, and the TMD as well as the last nine amino acids truncated CT of S. HEK293T cells were co-transfected with lentiviral packaging plasmids (pWPXL and pSPAX2) and GFP, GFP-CT or GFP-CT-Δ9, respectively. The cells were harvested and the virus-containing supernatants were collected and concentrated by ultracentrifugation at 48 h post transfection. The S protein expression levels in transfected cell **(B)** and concentrated lentiviral particles **(C)** were detected with Western blotting. GAPDH and Gag protein were used as internal controls. **(D)** Venn diagram illustrating the overlapping proteins interacting with GFP, GFP-CT or GFP-CT-ΔC9 in pseudovirus packaging cells identified using immunoprecipitation and mass spectrometry. Protein−protein interaction (PPI) network (**E**) and gene ontology (GO) analysis (**F**) of 35 proteins specifically interacting with GFP-CT. **(G)** HEK293T cells were transfected with the indicated siRNA using Lipofectamine RNAiMAX, followed by co-transfection with lentiviral packaging plasmids (pWPXL and psPAX2) and plasmid encoding full length S (FL-S) or the last nine amino acids truncated S (ΔC9) at 36 h after siRNA transfection. Lentiviral PSVs bearing FL-S or ΔC9 were harvested at 48 h after plasmids transfection and used to infect 293T-ACE2 cells. The luciferase activity in pseudovirus infected 293T-ACE2 cells was measured at 48 h post infection to assess the infectivity of pseudovirus and normalized to that of cells infected by pseudovirus from siNC-transfected cells. HEK293T cells were co-transfected with FLAG-tagged GFP, GFP-CT or GFP-CT-ΔC9 as well as plasmids encoding HA-tagged ARPC3, SCAMP3 or TUBB8 protein, respectively. The cell lysates were collected at 48 h post transfection and subjected to an immunoprecipitation assay using an anti-HA antibody. **(H)** The input and immunoprecipitated proteins were detected by Western blotting using anti-FLAG and anti-HA antibodies. (I) HEK293T cells were transfected with siRNA targeting ARPC3, SCAMP3 and TUBB8, respectively, followed by co-transfection with lentiviral packaging plasmids (pWPXL and psPAX2) and plasmid encoding full length S (FL-S) at 36 h after siRNA transfection. **(I)** Cells were harvested 48 h post plasmids transfection and the S protein expression level on the cell surface was assessed by flow cytometry using an anti-spike antibody and normalized to that of siNC-transfected cells. **(J)** Meanwhile, pseudovirus-containing supernatant was collected and concentrated by ultracentrifugation, and the S protein expression level in concentrated pseudovirus particles was detected with Western blotting. Gag protein was used as an internal control. Data are shown as the mean ± SEM (standard error of the mean) of at least three independent experiments. PSV, pseudovirus; ns, no significance; *, $p < 0.05$; **, $p < 0.01$; ***, $p < 0.001$.

lower than that in cells infected with FL-S packaged single-round infectious SARS-CoV-2, indicating that the deletion of the last 9 amino acids of the spike protein significantly inhibited the assembly of infectious SARS-CoV-2 virions (Fig. 5B). Moreover, knocking down ARPC3, SCAMP3 or TUBB8 remarkably suppressed the assembly of single-round infectious SARS-CoV-2 virions (Fig. 5C). These results suggest that the CT of the S protein and its interacting proteins may be promising targets for SARS-CoV-2 drug design.

Since the onset of the COVID-19 pandemic, many SARS-CoV-2 variants have arisen due to emerging mutations in the SARS-CoV-2 genome (Harvey et al., 2021). To investigate the impact of the CT of spike proteins on SARS-CoV-2 infection in the real world, we compared the frequency of mutations occurring in the CT of the spike protein. Notably, one mutation, V1264L, occurred at a particularly high frequency (Fig. 5D and Table S2). In general, an increase in the frequency of a mutation means that it may offer some selective advantage. Therefore, we firstly examined the effect of the V1264L mutation on the assembly of single-round infectious SARS-CoV-2. No significant difference in viral RNA expression levels was detected between the single-round infectious SARS-CoV-2 packaging cells transfected with wild-type spike protein (WT-S) and the V1264L mutant, indicating that V1264L mutation did not affect the replication of the SARS-CoV-2 genome (Fig. 5E). However, the expression levels of SARS-CoV-2 RNA in cells infected with V1264L-packaged single-round infectious SARS-CoV-2 were significantly higher than that in cells infected with WT-S-packaged single--round infectious SARS-CoV-2, suggesting that the V1264L mutation might facilitate the assembly of infectious SARS-CoV-2 virions (Fig. 5F). Furthermore, we examined the effect of the V1264L mutation on the packaging of SARS-CoV-2 PSV. The infectivity of the V1264L-packaged SARS-CoV-2 pseudovirus was obviously lower than that of the WT-S-packaged PSV (Fig. 5G). Although V1264L was expressed at the same level in PSV packaging cells as WT-S, its expression level in the pseudovirus particles was significantly lower than that of WT-S (Fig. 5H and I), suggesting that the V1264L mutation repressed the incorporation of spike protein into pseudovirus particles and resulted in decreased infectivity of SARS-CoV-2 pseudovirus. Additionally, this possibility was further demonstrated by comparing the subcellular localization of V1264L and WT-S by immunofluorescence assay (IFA) and flow cytometry. The IFA and flow cytometry results both showed that the V1264L mutation significantly reduced the localization of the S protein on the cell surface (Figs. 5J, 5K, and S3). Together, these results indicate that the V1264L mutation hampers the localization of the spike protein on the cell surface, thereby preventing the incorporation of spike protein into pseudovirus particles, but also promotes the intracellular localization of the spike protein accordingly and facilitates the assembly of infectious SARS-CoV-2 virions.

4. Discussion

Although the cytoplasmic tail (CT) of the viral envelope glycoprotein plays essential roles in multiple stages of viral infection, the function of the CT of the spike protein in the life cycle of SARS-CoV-2 is far from known. In this study, we identified the $V_{1264}L_{1265}$ motif in the CT of the SARS-CoV-2 and SARS-CoV spike proteins as a novel intracellular targeting signal that regulates the assembly of SARS-CoV-2 pseudovirus particles and live SARS-CoV-2 virions through modulating the intracellular transport and subcellular localization of the spike protein.

Previous studies have speculated that the deletion of the ER retrieval signal (ERRS) located in the C-terminus, KLHYT, increases localization of the spike protein on the cell surface and accounts for the increased infectivity of SARS-CoV and SARS-CoV-2 PSVs caused by the CT truncation. However, our results indicated that either deletion or mutation of the ERRS has no significant effect on promoting the cell surface localization of the SARS-CoV-2 S protein or the infectivity of the SARS-CoV-2 PSV (Figs. 1C and 2H). In addition, the deletion of the ERRS in the CT of HCoV-229E and HCoV-NL63 spike proteins did not improve the infectivity of the pseudovirus (Fig. S2). These results suggest that the ERRS in the CT of the spike protein might not be a key factor in the package of coronavirus PSVs. In sharp contrast, truncation of the last 9 amino acids of the CT of the S protein significantly promoted the cell surface localization of the spike protein and hence the infectivity of the pseudovirus, suggesting that the infectivity promotion of SARS-CoV and SARS-CoV-2 pseudoviruses caused by CT truncation of spike proteins is due to the disruption of the novel intracellular targeting signal, $V_{1264}L_{1265}$ motif, and not deletion of the ERRS. Our results provided new insight into how CT truncations of S protein increases the infectivity of SARS-CoV and SARS-CoV-2 PSVs.

Intracellular targeting signals of virus glycoproteins modulate their intracellular localization through interactions with vesicle coat proteins or related accessory proteins. For example, the KxHxx/KKxx motif interacts with coatomer complex I (COPI) to regulate proteins transport through the canonical secretory pathway (Jackson et al., 2012; McBride et al., 2007). The YxxΦ motif interacts with the clathrin complex including AP-1, AP-2, and AP-3 to mediate the intracellular transport of proteins (Bonifacino and Dell'Angelica, 1999; Bonifacino and Traub, 2003). A previous study suggested that there was a di-acidic ER export motif in the CT of SARS-CoV-2 spike protein, which interacted with COPII to modulate the intracellular trafficking of spike protein (Cattin-Ortola et al., 2021). In this study, we figured out that ARPC3, SCAMP3 and TUBB8 interact with the CT of SARS-CoV-2 spike protein and

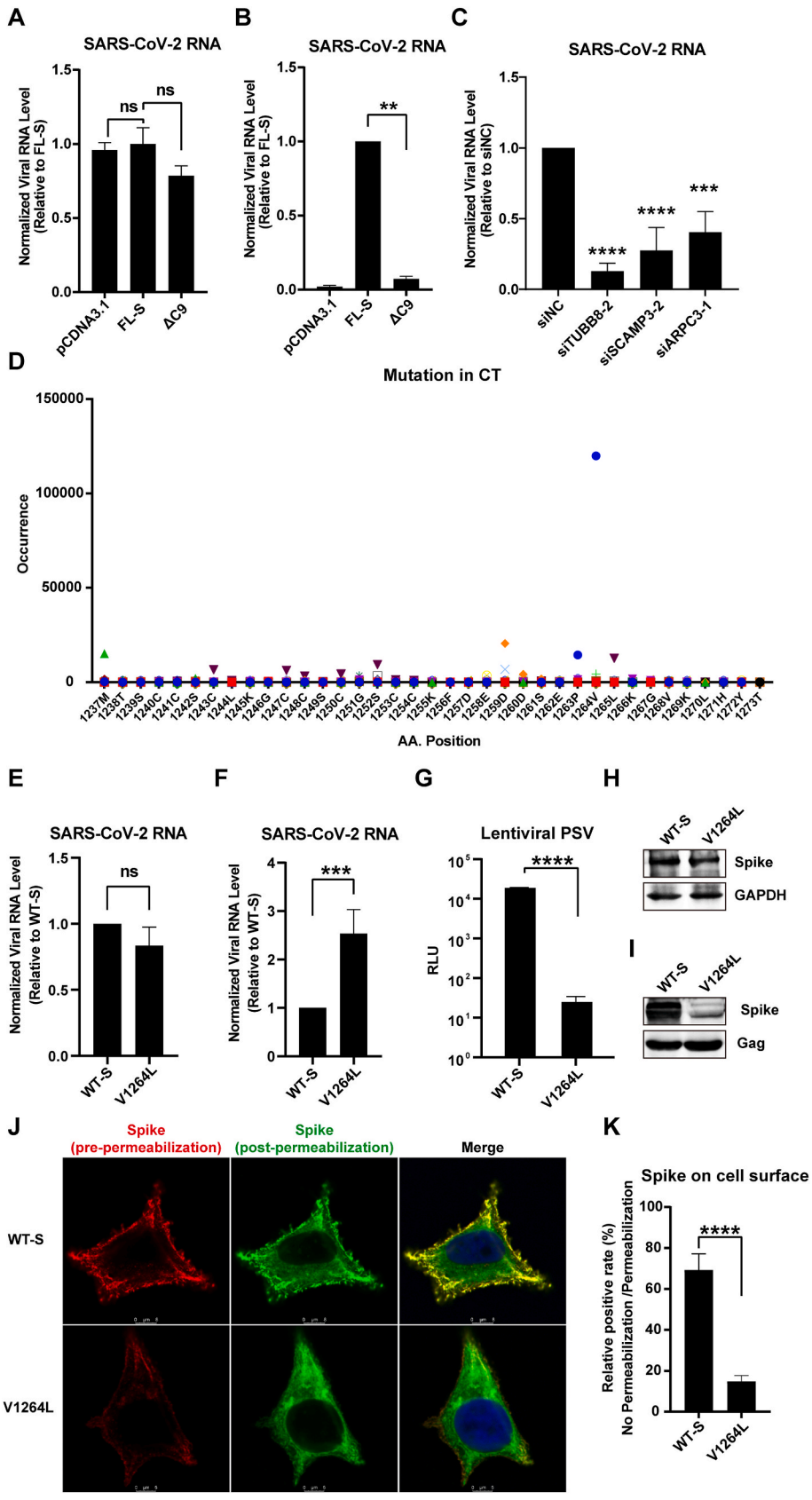

Fig. 5. $V_{1264}L_{1265}$ motif in the CT of the S protein modulated SARS-CoV-2 virion assembly. HEK293T cells were co-transfected with the SARS-CoV-2 replicon with the spike gene deleted and FL-S or ΔC9. **(A)** At 48 h post transfection, cells were harvested and viral RNA expression levels in transfected cells were measured by RT-qPCR and normalized to FL-S transfected cells. **(B)** Meanwhile, virus-containing supernatant was collected to infect 293T-ACE2 cells, and viral RNA expression levels in infected cells were measured by RT-qPCR, and normalized to FL-S transfected cells at 48 h post infection. **(C)** HEK293T cells were transfected with siRNA as indicated, followed by co-transfection with the SARS-CoV-2 replicon with the spike gene deleted and FL-S at 36 h post siRNA transfection. At 48 h post transfection, virus-containing supernatant was collected to infect 293T-ACE2 cells, and viral RNA expression levels in infected cells were measured by RT-qPCR, and normalized to siNC at 48 h post infection. **(D)** The frequency of mutations emerging in the cytoplasmic tail of the SARS-CoV-2 S protein in real world. Data were collected from the GISAID website in August 2022. **(E)** HEK293T cells were co-transfected with the SARS-CoV-2 replicon with the spike gene deleted and the FL-S or V1264L mutant. At 48 h post transfection, cells were harvested and viral RNA expression levels in transfected cells were measured by RT-qPCR, and normalized to FL-S transfected cells. **(F)** Meanwhile, virus-containing supernatant was collected to infect 293T-ACE2 cells, and viral RNA expression levels in infected cells were measured by RT-qPCR, and normalized to FL-S transfected cells at 48 h post infection. **(G)** Lentiviral SARS-CoV-2 pseudovirus carrying wild-type or V2164L mutant S protein was prepared and used to infect 293T-ACE2 cells. The luciferase activity in infected 293T-ACE2 cells was measured at 48 h post infection. The S protein expression levels in FL-S/V1264L transfected cells **(H)** and concentrated pseudovirus particles **(I)** were detected by Western blotting. GAPDH and gag were used as internal controls. **(J)** HeLa cells were transfected with plasmids expressing wild-type or V1264L mutant S protein, and immunofluorescence analysis (IFA) was performed to detect the cell surface and intracellular S protein. Scale bars: 10 μm. **(K)** HEK293T cells were transfected with plasmids expressing wild type or V1264L mutant S protein. Cells were harvested 48 h after transfection and cell surface expression of S protein in non-permeabilized cells, and total S expression in permeabilized cells was measured by flow cytometry. Data are shown as the mean ± SEM (standard error of the mean) of at least three independent experiments. PSV, pseudovirus; ns, no significance; *, $p < 0.05$; **, $p < 0.01$; ***, $p < 0.001$.

regulate intracellular transport of the spike protein. ARPC3 is one of the seven subunits of the actin-related protein complex (Arp2/3), which is involved in globular actin polymerization and essential for vesicle trafficking (Mu et al., 2016; Zhou et al., 2015). TUBB8 is a primate-specific β-tubulin isotype, whose physiological function has not been fully understood (Feng et al., 2016). So far, this is the first time that TUBB8 has been linked to viral infection. Previous studies have provided evidences supporting that the interaction between cytoskeleton and spike proteins is essential for coronavirus infection (Wen et al., 2020). For example, Ezrin, a membrane–actin linker, interacts with the CT of the SARS-CoV spike protein and impedes virus entry and fusion (Millet et al., 2012). The success assembly and release of infectious viral particles of HCoV-229E, HCoV-NL63 and transmissible gastroenteritis virus (TGEV) rely on the interactions between tubulins and S proteins (Rudiger et al., 2016). Nevertheless, the effect of the interaction between SARS-CoV-2 spike protein and cytoskeleton associated proteins on SARS-CoV-2 infection is unknown. Our results provide evidence for the participation of cytoskeleton related proteins ARPC3 and TUBB8, in regulating SARS-CoV-2 infection through modulating intracellular transport of the S protein. During SARS-CoV-2 infection, spike proteins are initially translated in the endoplasmic reticulum (ER) and then trafficked to the ER Golgi intermediate compartment (ERGIC) and later Golgi compartments where they are assembled into virions (V'Kovski et al., 2021). Additionally, some spike proteins are present on the cell surface via the secretory pathway. SCAMP3, a member of the secretory carrier membrane protein family, functions as a recycling carrier to the cell surface in post-Golgi recycling pathways and interacts with ESCRTs to regulate the process of multivesicular endosome biogenesis (Aoh et al., 2009; Falguieres et al., 2012). Although our results reveal that ARPC3, SCAMP3 and TUBB8 modulate the intracellular transport of S protein through interaction with the CT of S protein, the underlying mechanism by which these proteins modulate the transport of spike proteins remains to be further investigated. For instance, how SCAMP3, a recycling carrier to the cell surface, is involved in the intracellular transport of spike proteins? In addition, whether ARPC3, TUBB8 and SCAMP3 proteins individually or cooperatively regulate the transport of the spike protein? Further investigation is required to answer these questions.

Considering the high mutation rate of the extracellular domain of the SARS-CoV-2 S protein, the CT with low mutation rate and its corresponding host proteins are more attractive drug targets. Previous study has suggested that synthetic peptides corresponding to the CT of the S protein inhibit SARS-CoV-2 infection by blunting the interaction between the S protein and the N protein (Park et al., 2021). Moreover, inhibition of the Numb-associated kinases, which regulates intracellular membrane trafficking, effectively suppressed SARS-CoV-2 infection (Karim et al., 2022; Xiang et al., 2022b). Our results provided data that knocking down the expression of APRC3, SCAMP3, and TUBB8 significantly suppresses the assembly of the single-round infectious SARS-CoV-2 virions, suggesting that their important roles on SARS-CoV-2 infection or assembly (Fig. 5C). Consistent with this, two groups have also identified ARPC3 as a host factor required for SARS-CoV-2 infection using genome-wide CRISPR/Cas9 screening, which also verified our findings to a certain extent (Daniloski et al., 2021; Zhu et al., 2021). Therefore, all this has led to an interest in the possibility that the CT of the S protein, CT-interacting proteins, and the intercellular trafficking of S protein are potential targets for therapeutic strategies against SARS-CoV-2.

In conclusion, we identified $V_{1264}L_{1265}$ as a new intracellular targeting signal in the CT of the spike protein of SARS-CoV-2 that regulates the intracellular transport and subcellular localization of the spike protein through interactions with cytoskeleton and vesicular transport-related proteins, and thereby affects the packaging of SARS-CoV-2 pseudovirus and live SARS-CoV-2. Our study extends the understanding of the role of CT of the S protein in the SARS-CoV-2 infection and provides potential strategies for the treatment of SARS-CoV-2 infection.

Declaration of competing interest

The authors declare that they have no known competing financial interests or personal relationships that could have appeared to influence the work reported in this paper.

Data availability

Data will be made available on request.

Acknowledgement

This research was funded by the Natural Science Foundation of Guangdong Province (2019A1515011681 for LB.H.); Guangzhou Medical University Discipline Construction Funds (Basic Medicine, JCXKJS2022A11 for L.H.); the National 111 Project (D18010); Guangdong key research and development project (2022B1111020004 & 2022B1111020005), and Guangzhou Innovation and Entrepreneurship Leading Team Grant (CYLJTD-201602).

Appendix A. Supplementary data

Supplementary data to this article can be found online at https://doi.org/10.1016/j.antiviral.2022.105509.

References

Aoh, Q.L., Castle, A.M., Hubbard, C.H., Katsumata, O., Castle, J.D., 2009. SCAMP3 negatively regulates epidermal growth factor receptor degradation and promotes receptor recycling. Mol. Biol. Cell 20, 1816–1832.
Bai, C., Zhong, Q., Gao, G.F., 2022. Overview of SARS-CoV-2 genome-encoded proteins. Sci. China Life Sci. 65, 280–294.
Barman, S., Adhikary, L., Chakrabarti, A.K., Bernas, C., Kawaoka, Y., Nayak, D.P., 2004. Role of transmembrane domain and cytoplasmic tail amino acid sequences of influenza a virus neuraminidase in raft association and virus budding. J. Virol. 78, 5258–5269.
Baviskar, P.S., Hotard, A.L., Moore, M.L., Oomens, A.G., 2013. The respiratory syncytial virus fusion protein targets to the perimeter of inclusion bodies and facilitates filament formation by a cytoplasmic tail-dependent mechanism. J. Virol. 87, 10730–10741.
Bonifacino, J.S., Dell'Angelica, E.C., 1999. Molecular bases for the recognition of tyrosine-based sorting signals. J. Cell Biol. 145, 923–926.
Bonifacino, J.S., Traub, L.M., 2003. Signals for sorting of transmembrane proteins to endosomes and lysosomes. Annu. Rev. Biochem. 72, 395–447.
Broer, R., Boson, B., Spaan, W., Cosset, F.L., Corver, J., 2006. Important role for the transmembrane domain of severe acute respiratory syndrome coronavirus spike protein during entry. J. Virol. 80, 1302–1310.
Cattin-Ortola, J., Welch, L.G., Maslen, S.L., Papa, G., James, L.C., Munro, S., 2021. Sequences in the cytoplasmic tail of SARS-CoV-2 Spike facilitate expression at the cell surface and syncytia formation. Nat. Commun. 12, 5333.
Chen, H.Y., Huang, C., Tian, L., Huang, X., Zhang, C., Llewellyn, G.N., Rogers, G.L., Andresen, K., O'Gorman, M.R.G., Chen, Y.W., Cannon, P.M., 2021. Cytoplasmic tail truncation of SARS-CoV-2 Spike protein enhances titer of pseudotyped vectors but masks the effect of the D614G mutation. J. Virol., JVI0096621
Chen, M., Zhang, X.E., 2021. Construction and applications of SARS-CoV-2 pseudoviruses: a mini review. Int. J. Biol. Sci. 17, 1574–1580.
Corver, J., Broer, R., van Kasteren, P., Spaan, W., 2009. Mutagenesis of the transmembrane domain of the SARS coronavirus spike glycoprotein: refinement of the requirements for SARS coronavirus cell entry. Virol. J. 6, 230.
Daniloski, Z., Jordan, T.X., Wessels, H.H., Hoagland, D.A., Kasela, S., Legut, M., Maniatis, S., Mimitou, E.P., Lu, L., Geller, E., Danziger, O., Rosenberg, B.R., Phatnani, H., Smibert, P., Lappalainen, T., tenOever, B.R., Sanjana, N.E., 2021. Identification of required host factors for SARS-CoV-2 infection in human cells. Cell 184, 92–105 e116.
Elbe, S., Buckland-Merrett, G., 2017. Data, disease and diplomacy: GISAID's innovative contribution to global health. Glob. Chall. 1, 33–46.
Falguieres, T., Castle, D., Gruenberg, J., 2012. Regulation of the MVB pathway by SCAMP3. Traffic 13, 131–142.
Feng, R., Sang, Q., Kuang, Y., Sun, X., Yan, Z., Zhang, S., Shi, J., Tian, G., Luchniak, A., Fukuda, Y., Li, B., Yu, M., Chen, J., Xu, Y., Guo, L., Qu, R., Wang, X., Sun, Z., Liu, M., Shi, H., Wang, H., Feng, Y., Shao, R., Chai, R., Li, Q., Xing, Q., Zhang, R., Nogales, E., Jin, L., He, L., Gupta Jr., M.L., Cowan, N.J., Wang, L., 2016. Mutations in TUBB8 and human oocyte meiotic arrest. N. Engl. J. Med. 374, 223–232.
Freed, E.O., 2015. HIV-1 assembly, release and maturation. Nat. Rev. 13, 484–496.
Giroglou, T., Cinatl Jr., J., Rabenau, H., Drosten, C., Schwalbe, H., Doerr, H.W., von Laer, D., 2004. Retroviral vectors pseudotyped with severe acute respiratory syndrome coronavirus S protein. J. Virol. 78, 9007–9015.

Harvey, W.T., Carabelli, A.M., Jackson, B., Gupta, R.K., Thomson, E.C., Harrison, E.M., Ludden, C., Reeve, R., Rambaut, A., Consortium, C.-G.U., Peacock, S.J., Robertson, D.L., 2021. SARS-CoV-2 variants, spike mutations and immune escape. Nat. Rev. 19, 409–424.

Hou, Y., Meulia, T., Gao, X., Saif, L.J., Wang, Q., 2019. Deletion of both the tyrosine-based endocytosis signal and the endoplasmic reticulum retrieval signal in the cytoplasmic tail of spike protein attenuates porcine epidemic diarrhea virus in pigs. J. Virol. 93.

Hu, L., Xu, Y., Wu, L., Feng, J., Zhang, L., Tang, Y., Zhao, X., Mai, R., Chen, L., Mei, L., Tan, Y., Du, Y., Zhen, Y., Su, W., Peng, T., 2022. The E484K substitution in a SARS-CoV-2 spike protein subunit vaccine resulted in limited cross-reactive neutralizing antibody responses in mice. Viruses 14.

Jackson, L.P., Lewis, M., Kent, H.M., Edeling, M.A., Evans, P.R., Duden, R., Owen, D.J., 2012. Molecular basis for recognition of dilysine trafficking motifs by COPI. Dev. Cell 23, 1255–1262.

Jennings, B.C., Kornfeld, S., Doray, B., 2021. A weak COPI binding motif in the cytoplasmic tail of SARS-CoV-2 spike glycoprotein is necessary for its cleavage, glycosylation, and localization. FEBS Lett. 595, 1758–1767.

Jin, H., Leser, G.P., Zhang, J., Lamb, R.A., 1997. Influenza virus hemagglutinin and neuraminidase cytoplasmic tails control particle shape. EMBO J. 16, 1236–1247.

Jin, Y.Y., Lin, H., Cao, L., Wu, W.C., Ji, Y., Du, L., Jiang, Y., Xie, Y., Tong, K., Xing, F., Zheng, F., Shi, M., Pan, J.A., Peng, X., Guo, D., 2021. A convenient and biosafe replicon with accessory genes of SARS-CoV-2 and its potential application in antiviral drug discovery. Virol. Sin. 36, 913–923.

Johnson, M.C., Lyddon, T.D., Suarez, R., Salcedo, B., LePique, M., Graham, M., Ricana, C., Robinson, C., Ritter, D.G., 2020. Optimized pseudotyping conditions for the SARS-COV-2 spike glycoprotein. J. Virol. 94.

Karim, M., Saul, S., Ghita, L., Sahoo, M.K., Ye, C., Bhalla, N., Lo, C.W., Jin, J., Park, J.G., Martinez-Gualda, B., East, M.P., Johnson, G.L., Pinsky, B.A., Martinez-Sobrido, L., Asquith, C.R.M., Narayanan, A., De Jonghe, S., Einav, S., 2022. Numb-associated kinases are required for SARS-CoV-2 infection and are cellular targets for antiviral strategies. Antivir. Res. 204, 105367.

Kordyukova, L.V., Konarev, P.V., Fedorova, N.V., Shtykova, E.V., Ksenofontov, A.L., Loshkarev, N.A., Dadinova, L.A., Timofeeva, T.A., Abramchuk, S.S., Moiseenko, A.V., Baratova, L.A., Svergun, D.I., Batishchev, O.V., 2021. The cytoplasmic tail of influenza A virus hemagglutinin and membrane lipid composition change the mode of M1 protein association with the lipid bilayer. Membranes 11.

Lebeau, G., Vagner, D., Frumence, E., Ah-Pine, F., Guillot, X., Nobecourt, E., Raffray, L., Gasque, P., 2020. Deciphering SARS-CoV-2 virologic and immunologic features. Int. J. Mol. Sci. 21.

Lontok, E., Corse, E., Machamer, C.E., 2004. Intracellular targeting signals contribute to localization of coronavirus spike proteins near the virus assembly site. J. Virol. 78, 5913–5922.

Lyles, D.S., 2013. Assembly and budding of negative-strand RNA viruses. Adv. Virus Res. 85, 57–90.

McBride, C.E., Li, J., Machamer, C.E., 2007. The cytoplasmic tail of the severe acute respiratory syndrome coronavirus spike protein contains a novel endoplasmic reticulum retrieval signal that binds COPI and promotes interaction with membrane protein. J. Virol. 81, 2418–2428.

Millet, J.K., Kien, F., Cheung, C.Y., Siu, Y.L., Chan, W.L., Li, H., Leung, H.L., Jaume, M., Bruzzone, R., Peiris, J.S., Altmeyer, R.M., Nal, B., 2012. Ezrin interacts with the SARS coronavirus Spike protein and restrains infection at the entry stage. PLoS One 7, e49566.

Moore, M.J., Dorfman, T., Li, W., Wong, S.K., Li, Y., Kuhn, J.H., Coderre, J., Vasilieva, N., Han, Z., Greenough, T.C., Farzan, M., Choe, H., 2004. Retroviruses pseudotyped with the severe acute respiratory syndrome coronavirus spike protein efficiently infect cells expressing angiotensin-converting enzyme 2. J. Virol. 78, 10628–10635.

Mu, J., Zhang, Y., Hu, Y., Hu, X., Zhou, Y., Chen, X., Wang, Y., 2016. The role of viral protein Ac34 in nuclear relocation of subunits of the actin-related protein 2/3 complex. Virol. Sin. 31, 480–489.

Muranyi, W., Malkusch, S., Muller, B., Heilemann, M., Krausslich, H.G., 2013. Super-resolution microscopy reveals specific recruitment of HIV-1 envelope proteins to viral assembly sites dependent on the envelope C-terminal tail. PLoS Pathog. 9, e1003198.

Nie, J., Li, Q., Wu, J., Zhao, C., Hao, H., Liu, H., Zhang, L., Nie, L., Qin, H., Wang, M., Lu, Q., Li, X., Sun, Q., Liu, J., Fan, C., Huang, W., Xu, M., Wang, Y., 2020. Establishment and validation of a pseudovirus neutralization assay for SARS-CoV-2. Emerg. Microb. Infect. 9, 680–686.

Park, B.K., Kim, J., Park, S., Kim, D., Kim, M., Baek, K., Bae, J.Y., Park, M.S., Kim, W.K., Lee, Y., Kwon, H.J., 2021. MERS-CoV and SARS-CoV-2 replication can be inhibited by targeting the interaction between the viral spike protein and the nucleocapsid protein. Theranostics 11, 3853–3867.

Peng, T., 2010. Strategies for antiviral screening targeting early steps of virus infection. Virol. Sin. 25, 281–293.

Postler, T.S., Desrosiers, R.C., 2013. The tale of the long tail: the cytoplasmic domain of HIV-1 gp41. J. Virol. 87, 2–15.

Ricardo-Lax, I., Luna, J.M., Thao, T.T.N., Le Pen, J., Yu, Y., Hoffmann, H.H., Schneider, W.M., Razooky, B.S., Fernandez-Martinez, J., Schmidt, F., Weisblum, Y., Trueb, B.S., Berenguer Veiga, I., Schmied, K., Ebert, N., Michailidis, E., Peace, A., Sanchez-Rivera, F.J., Lowe, S.W., Rout, M.P., Hatziioannou, T., Bieniasz, P.D., Poirier, J.T., MacDonald, M.R., Thiel, V., Rice, C.M., 2021. Replication and single-cycle delivery of SARS-CoV-2 replicons. Science 374, 1099–1106.

Roy, N.H., Chan, J., Lambele, M., Thali, M., 2013. Clustering and mobility of HIV-1 Env at viral assembly sites predict its propensity to induce cell-cell fusion. J. Virol. 87, 7516–7525.

Rudiger, A.T., Mayrhofer, P., Ma-Lauer, Y., Pohlentz, G., Muthing, J., von Brunn, A., Schwegmann-Wessels, C., 2016. Tubulins interact with porcine and human S proteins of the genus Alphacoronavirus and support successful assembly and release of infectious viral particles. Virology 497, 185–197.

Sachs, J.D., Karim, S.S.A., Aknin, L., Allen, J., Brosbol, K., Colombo, F., Barron, G.C., Espinosa, M.F., Gaspar, V., Gaviria, A., Haines, A., Hotez, P.J., Koundouri, P., Bascunan, F.L., Lee, J.K., Pate, M.A., Ramos, G., Reddy, K.S., Serageldin, I., Thwaites, J., Vike-Freiberga, V., Wang, C., Were, M.K., Xue, L., Bahadur, C., Bottazzi, M.E., Bullen, C., Laryea-Adjei, G., Amor, Y.B., Karadag, O., Lafortune, G., Torres, E., Barredo, L., Bartels, J.G.E., Joshi, N., Hellard, M., Huynh, U.K., Khandelwal, S., Lazarus, J.V., Michie, S., 2022. The Lancet Commission on lessons for the future from the COVID-19 pandemic. Lancet 400, 1224–1280.

Salazar-Garcia, M., Acosta-Contreras, S., Rodriguez-Martinez, G., Cruz-Rangel, A., Flores-Alanis, A., Patino-Lopez, G., Luna-Pineda, V.M., 2021. Pseudotyped vesicular stomatitis virus-severe acute respiratory syndrome-coronavirus-2 spike for the study of variants, vaccines, and therapeutics against coronavirus disease 2019. Front. Microbiol. 12, 817200.

Shaikh, F.Y., Cox, R.G., Lifland, A.W., Hotard, A.L., Williams, J.V., Moore, M.L., Santangelo, P.J., Crowe Jr., J.E., 2012. A critical phenylalanine residue in the respiratory syncytial virus fusion protein cytoplasmic tail mediates assembly of internal viral proteins into viral filaments and particles. mBio 3.

Tedbury, P.R., Freed, E.O., 2015. The cytoplasmic tail of retroviral envelope glycoproteins. Prog. Mol. Biol. Transl. Sci. 129, 253–284.

Ujike, M., Huang, C., Shirato, K., Makino, S., Taguchi, F., 2016. The contribution of the cytoplasmic retrieval signal of severe acute respiratory syndrome coronavirus to intracellular accumulation of S proteins and incorporation of S protein into virus-like particles. J. Gen. Virol. 97, 1853–1864.

V'Kovski, P., Kratzel, A., Steiner, S., Stalder, H., Thiel, V., 2021. Coronavirus biology and replication: implications for SARS-CoV-2. Nat. Rev. 19, 155–170.

Wen, Z., Zhang, Y., Lin, Z., Shi, K., Jiu, Y., 2020. Cytoskeleton-a crucial key in host cell for coronavirus infection. J. Mol. Cell Biol. 12, 968–979.

Xiang, Q., Li, L., Wu, J., Tian, M., Fu, Y., 2022a. Application of pseudovirus system in the development of vaccine, antiviral-drugs, and neutralizing antibodies. Microbiol. Res. 258, 126993.

Xiang, R., Yu, Z., Wang, Y., Wang, L., Huo, S., Li, Y., Liang, R., Hao, Q., Ying, T., Gao, Y., Yu, F., Jiang, S., 2022b. Recent advances in developing small-molecule inhibitors against SARS-CoV-2. Acta Pharm. Sin. B 12, 1591–1623.

Yu, J., Li, Z., He, X., Gebre, M.S., Bondzie, E.A., Wan, H., Jacob-Dolan, C., Martinez, D.R., Nkolola, J.P., Baric, R.S., Barouch, D.H., 2021. Deletion of the SARS-CoV-2 spike cytoplasmic tail increases infectivity in pseudovirus neutralization assays. J. Virol. 95, e00044-21.

Zhou, K., Sumigray, K.D., Lechler, T., 2015. The Arp2/3 complex has essential roles in vesicle trafficking and transcytosis in the mammalian small intestine. Mol. Biol. Cell 26, 1995–2004.

Zhu, Y., Feng, F., Hu, G., Wang, Y., Yu, Y., Zhu, Y., Xu, W., Cai, X., Sun, Z., Han, W., Ye, R., Qu, D., Ding, Q., Huang, X., Chen, H., Xu, W., Xie, Y., Cai, Q., Yuan, Z., Zhang, R., 2021. A genome-wide CRISPR screen identifies host factors that regulate SARS-CoV-2 entry. Nat. Commun. 12, 961.